Three-body halos. III. Effects of finite core spin

D.V. Fedorov*
Institute of Physics and Astronomy, Aarhus University, DK-8000 Aarhus C, Denmark
and European Centre for Theoretical Studies in Nuclear Physics and Related Areas, I-38050 Trento, Italy

E. Garrido and A.S. Jensen
Institute of Physics and Astronomy, Aarhus University, DK-8000 Aarhus C, Denmark
(Received 18 January 1995)

We investigate effects of finite core spin in two-neutron halos in the three-body model consisting of two neutrons and a core. The states in the neutron-core subsystem can then have an additional splitting due to the coupling of the neutron and core spins. The connection between the structure of the total system and the states of the neutron-core subsystem depends strongly on this spin splitting. However, the spatial structure is essentially unchanged. The neutron momentum distribution in a nuclear dissociation reaction will consist of a broad and a narrow distribution arising from the two spin split neutron-core virtual states. The large distance behavior is investigated and the conditions for the Efimov effect turn out to be more restrictive. The magnetic moment is equal to the core value independent of spin splitting and energies of the neutron-core states. The excited states of opposite parity depend strongly on the spin splitting. The parameters in our numerical examples are chosen to be appropriate for ^{11}Li and ^{19}B.

PACS number(s): 21.45.+v, 21.60.Gx

I. INTRODUCTION

The existence of halo nuclei is by now established [1–3] as weakly bound and spatially extended systems. A rather accurate description is obtained by use of two- and three-body models. Criteria for the occurrence of halos and the related asymptotic large distance behavior were recently discussed [4–7]. These investigations assumed many simplifying approximations, which allowed extraction of general properties and therefore provided insight into the general nature of such systems. Of particular interest are bound three-body systems where furthermore all two-particle subsystems are unbound. These so-called Borromean systems [8] appear for a substantial range of two-body potentials [9].

The nucleus ^{11}Li has played an especially dominating role in the developments. The approximate description as a three-body system consisting of two neutrons outside the ^{9}Li-core was only recently suggested [10–12]. Since then a series of improved calculations appeared, see for example [8]. The most detailed and accurate of these three-body computations are based on the Faddeev equations [13]. In spite of the large number of publications the possibly significant consequences of the finite core-spin s_c has so far not been considered at all in three-body calculations. The neutron and the core spins can couple to a total angular momentum of $s_c \pm \frac{1}{2}$, while the neutron-core motion still remains in the same relative orbital state. If the interaction is independent of these couplings, the structure corresponds to that of a spin-zero core. This is, however, highly improbable considering the well-known appreciable spin dependence both of the strong interaction and of the observed bound states and resonances throughout the periodic table. The states in neighboring nuclei like ^{12}B, ^{12}N, and ^{8}Li as well as computations are in particular suggestive for a similar spin splitting in ^{10}Li, see [14,15].

The purpose of this paper is to investigate the consequences of finite core spin for halo nuclei. The resulting spin splitting is probably an important ingredient for understanding the relation between the ground-state structures of the neutron-core subsystem and the total three-body system, e.g, ^{10}Li and ^{11}Li. Another effect is that the peculiar Efimov structure [16], which might show up in halo nuclei, is hindered by the spin splitting of the virtual s states. As in our earlier papers [4,6,7] we want to establish the general features, qualitatively or quantitatively as best we can, and apply the results on realistic examples. We shall again for convenience assume that all three particles are inert and all the core degrees of freedom are therefore frozen. We shall furthermore assume throughout the paper that the total angular momentum J for the ground state is equal to s_c and that the total parity equals that of the core.

This paper is the third (after [6,7]) in a series of papers discussing various aspects of three-body halos. After the Introduction we sketch in Sec. II the general theoretical method used to compute the properties of the three-body system. The interactions between the different two-body subsystems are parametrized in Sec. III. In Sec. IV the asymptotic form of the Faddeev equations is derived for interactions causing the spin splitting and in Sec. V is discussed the large distance behavior in connection with

*On leave from the Kurchatov Institute, 123182 Moscow, Russia.

 ©1995 The American Physical Society

the Efimov effect. The resulting spatial structure and the measured momentum distributions are discussed in Sec. VI. Magnetic moment is investigated in Sec. VII and excited states of 1^- character on top of the ground state in Sec. VIII. Finally we give a summary and the conclusions in Sec IX.

II. METHOD

The Hamiltonian of the system, where the center-of-mass kinetic energy is subtracted, is given by

$$H = \sum_{i=1}^{3} \frac{p_i^2}{2m_i} - \frac{P^2}{2M} + \sum_{i>j=1}^{3} V_{ij} \ , \tag{1}$$

where m_i, $\mathbf{r}_i$, and $\mathbf{p}_i$ are mass, coordinate, and momentum of the ith particle, V_{ij} are the two-body potentials, P and M are, respectively, the total momentum and the total mass of the system. We shall use the Jacobi coordinates basically defined as the relative coordinates between two of the particles ($\mathbf{x}$) and between their center of mass and the third particle ($\mathbf{y}$). The precise definitions and the corresponding three sets of hyperspherical coordinates (ρ,α,Ω_x, Ω_y) are elsewhere defined, see e.g. [6–8]. Here ρ ($= \sqrt{x^2 + y^2}$) is the generalized radial coordinate and α, in the interval $[0, \pi/2]$, defines the relative size of $\mathbf{x}$ and $\mathbf{y}$, Ω_x and Ω_y are the angles describing the directions of $\mathbf{x}$ and $\mathbf{y}$. One of these sets of hyperspherical coordinates is in principle sufficient for a complete description. The volume element is given by $\rho^5 d\Omega\, d\rho$ where $d\Omega = \sin^2\alpha \cos^2\alpha\, d\alpha\, d\Omega_x d\Omega_y$.

The total wave function Ψ of the three-body system is written as a sum of three components each expressed in terms of one of the three different sets of Jacobi coordinates:

$$\Psi = \sum_{i=1}^{3} \psi^{(i)}(\mathbf{x}_i, \mathbf{y}_i). \tag{2}$$

This three-component wave function is flexible and allows a description of different three-body structures by means of rather few angular momenta in each component. These wave functions satisfy the three Faddeev equations [13]

$$(T - E)\psi^{(i)} + V_{jk}(\psi^{(i)} + \psi^{(j)} + \psi^{(k)}) = 0, \tag{3}$$

where E is the total energy, T is the kinetic energy operator, and $\{i, j, k\}$ is a cyclic permutation of $\{1, 2, 3\}$. Any solution to Eq. (3) is via Eq. (2) also a solution to the Schrödinger equation, but the Faddeev equations, which in practice almost inevitably appear as integro-differential equations, are much better suited for descriptions of delicate correlations.

Each component $\psi^{(i)}$ is now for each ρ expanded in a complete set of generalized angular functions $\Phi_n^{(i)}(\rho, \Omega_i)$.

$$\psi^{(i)} = \frac{1}{\rho^{5/2}} \sum_n f_n(\rho) \Phi_n^{(i)}(\rho, \Omega_i) \ , \tag{4}$$

where $\rho^{-5/2}$ is the phase-space factor. The angular functions must be chosen to describe correctly the asymptotic behavior of the wave function and in particular the behavior corresponding to possible bound two-body subchannels. This is essential for low energies where the correlations must be described very accurately. These functions are now chosen for each ρ as the eigenfunctions of the angular part of the Faddeev equations:

$$\frac{\hbar^2}{2m}\frac{1}{\rho^2}\hat{\Lambda}^2 \Phi_n^{(i)} + V_{jk}(\Phi_n^{(i)} + \Phi_n^{(j)} + \Phi_n^{(k)}) \equiv \frac{\hbar^2}{2m}\frac{1}{\rho^2}\lambda_n(\rho)\Phi_n^{(i)}, \tag{5}$$

where $\{i, j, k\}$ again is a cyclic permutation of $\{1, 2, 3\}$ and $\hat{\Lambda}^2$ is the ρ-independent part of the kinetic energy operator defined by

$$T \equiv T_\rho + \frac{\hbar^2}{2m}\frac{1}{\rho^2}\hat{\Lambda}^2, \qquad T_\rho = -\frac{\hbar^2}{2m}\left(\rho^{-5/2}\frac{\partial^2}{\partial\rho^2}\rho^{5/2} - \frac{1}{\rho^2}\frac{15}{4}\right) . \tag{6}$$

Explicitly the generalized angular momentum operator $\hat{\Lambda}^2$ is given by

$$\hat{\Lambda}^2 = -\frac{1}{\sin\alpha\cos\alpha}\frac{\partial^2}{\partial\alpha^2}\sin\alpha\cos\alpha + \frac{\hat{l}_x^2}{\sin^2\alpha} + \frac{\hat{l}_y^2}{\cos^2\alpha} - 4 \tag{7}$$

in terms of the angular momentum operators $\hat{l}_x^2$ and $\hat{l}_y^2$ related to the $\mathbf{x}$ and $\mathbf{y}$ degrees of freedom. This procedure is particularly convenient, since all angular variables are confined to finite parameter intervals and therefore correspond to discrete eigenvalue spectra. The idea, here applied to the Faddeev equations, was exploited previously to solve the Schrödinger equation in atomic physics [17] and recently also in studies of the triton [18].

The radial expansion coefficients $f_n(\rho)$ are component independent, since ρ is independent of which Jacobi coordinates are used. Insertion of Eq. (4) into Eq. (3) and use of Eqs. (5), (6), and (7) then lead to the following coupled set of "radial" differential equations:

$$\left[-\frac{d^2}{d\rho^2} - \frac{2mE}{\hbar^2} + \frac{1}{\rho^2}\left(\lambda_n(\rho) + \frac{15}{4}\right)\right] f_n + \sum_{n'}\left(-2P_{nn'}\frac{d}{d\rho} - Q_{nn'}\right) f_{n'} = 0, \tag{8}$$

where the functions P and Q are the following angular integrals:

$$P_{nn'}(\rho) \equiv \sum_{i,j=1}^{3} \int d\Omega\, \Phi_n^{(i)*}(\rho, \Omega)\frac{\partial}{\partial\rho}\Phi_{n'}^{(j)}(\rho, \Omega), \tag{9}$$

$$Q_{nn'}(\rho) \equiv \sum_{i,j=1}^{3} \int d\Omega\, \Phi_n^{(i)*}(\rho, \Omega)\frac{\partial^2}{\partial\rho^2}\Phi_{n'}^{(j)}(\rho, \Omega). \tag{10}$$

Often very few terms of the expansion in Eq. (4) is needed to get sufficient accuracy in calculations of the lowest-lying states. On the other hand the method is not suited for highly excited states where many high angular momenta are needed in the expansion. Systems with many crossings of the λ values as function of ρ are also numerically difficult to solve accurately by this method.

III. TWO-BODY POTENTIALS

Loosely bound systems are mainly sensitive to the low-energy properties of the potentials and we shall therefore use relatively simple potentials reproducing the available low-energy scattering data and still allowing extensive three-body calculations. The neutron-neutron interaction in the singlet s wave is assumed to be the same as in Ref. [10], where the radial shape is a Gaussian. In the extension to triplet p waves we include spin-spin, spin-orbit, and tensor terms. The resulting potential is then

$$V_{nn} = \Big(V_c + V_{\rm ss}\mathbf{s}_{n1}\cdot\mathbf{s}_{n2} + V_T\hat{S}_{12} + V_{\rm so}\mathbf{l}_{nn}\cdot\mathbf{s}_{nn} \Big) \exp[-(r/b_{nn})^2], \quad (11)$$

where $\mathbf{s}_{n1}$ and $\mathbf{s}_{n2}$ are the spins of the neutrons, $\mathbf{s}_{nn} = \mathbf{s}_{n1} + \mathbf{s}_{n2}$, and $\hat{S}_{12}$ is the usual tensor operator. The four strength parameters and the range of the Gaussian are then adjusted to reproduce the following four scattering lengths a and the s-wave effective range r_e [19]:

$$a(^1S_0) = 18.8 \text{ fm},\ r_e(^1S_0) = 2.76 \text{ fm},$$
$$a(^3P_0) = 3.6 \text{ fm},\ a(^3P_1) = -2.0 \text{ fm},\ a(^3P_2) = 0.30 \text{ fm}. \quad (12)$$

The resulting values are given by

$$V_c = 2.92 \text{ MeV},\ V_{\rm ss} = 45.22 \text{ MeV},\ V_T = 26.85 \text{ MeV},$$
$$V_{\rm so} = -12.08 \text{ MeV},\ b_{nn} = 1.8 \text{ fm}, \quad (13)$$

which by use in Eq. (12) leads to the proper low-energy behavior both in the s wave and the three different p waves.

The neutron-core potential, which also is assumed to have a Gaussian radial shape, is directly related to the resonances or virtual states in the subsystem. Their positions in energy are crucial in the computations and it is necessary to be able to adjust s, p, and d waves independently. We therefore use the parametrization

$$V_{nc}^{(s)} = V_s(1+\gamma_s\mathbf{s}_c\cdot\mathbf{s}_n)\exp[-(r/b_{nc})^2],$$
$$V_{nc}^{(l)} = (V_l + V_{\rm so}^{(l)}\mathbf{s}_n\cdot\mathbf{l}_{nc})\exp[-(r/b_{nc})^2], \quad (14)$$

where $l = 1, 2$ corresponds to either p or d waves, $V_s, V_l, V_{\rm so}^{(l)}, \gamma_s$, and $b_{nc}(=2.55$ fm) are constants and $\mathbf{s}_c, \mathbf{s}_n$, and $\mathbf{l}_{nc}$ are the spin of the core, spin of the neutron, and the relative neutron-core orbital angular momentum. The spin splitting is for simplicity only introduced in the s state, but could as well be important for the other partial waves. Both the spin-orbit partners of higher orbital angular momenta may be independently adjusted. These effective potentials must take into account that the orbits occupied by the neutrons in the core are excluded by the Pauli principle. This is either done by choosing shallow potentials unable to hold bound states or by considering higher lying three-body states.

We first choose [10] $V_s = V_p = -7.8$ MeV, $V_{\rm so}^{(l)} = 0$, and $\gamma_s = 0$, which results in a total binding energy of 0.3 MeV corresponding to ^{11}Li. Maintaining this binding energy of the three-body system and varying V_s and $V_{\rm so}$, we obtain the curve in Fig. 1 relating the virtual $s_{1/2}$ state and the $p_{1/2}$ resonance in the neutron-core system. When one of these states is very low the corresponding component is dominating in the three-body wave function. The straight lines between the calculated points are inserted to guide the eye.

The spin splitting is now investigated by varying γ_s and V_s while keeping the binding energy at 0.3 MeV and $V_{\rm so}$ at the values corresponding to the square and the vertical line in Fig. 1. The resulting connection between the virtual s states are shown in Fig. 2 for these two cases. When the energy of one of the states increases the other decreases due to the inherent coupling in the Faddeev equations. A finite p-state admixture (the squares) increases the energies of the virtual s states to maintain the total binding energy. In both cases the energy of one of the spin-split virtual s states in the neutron-core system may occur anywhere below 0.1 MeV.

The angular momentum dependence is now investigated by using a $d_{5/2}$ resonance instead of the $p_{1/2}$ resonance in the neutron-core system. This might be the relevant structure for ^{19}B, where the ^{17}B core probably has an essentially fully occupied p shell. The total angular momentum of ^{17}B is 3/2 which also is the expected

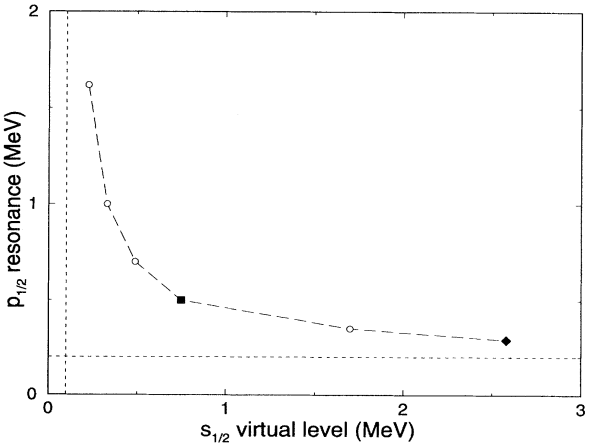

FIG. 1. The relation between the virtual $s_{1/2}$ state and the $p_{1/2}$ resonance for a total binding energy of 0.30 MeV. The curve is obtained by varying V_s and $V_{\rm so}^{(s)}$ while keeping $V_p = -7.8$ MeV and $\gamma_s = 0$. The square, the diamond, and the dashed lines (corresponding to the asymptotic values) indicate points of interest in the following figures.

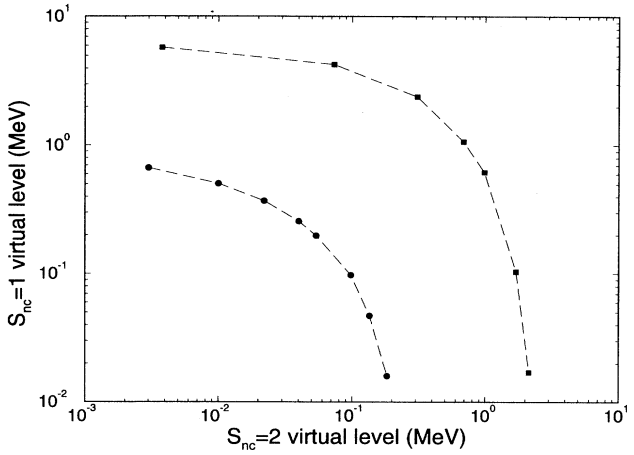

FIG. 2. The relation between the two virtual s states (total neutron-core spin $S_{nc} = 1, 2$) for a total binding energy of 0.30 MeV for ^{11}Li. The curves are obtained by varying V_s and γ_s while the other interaction parameters are defined by the points indicated in Fig. 1 by the vertical line (circles) and the square (squares).

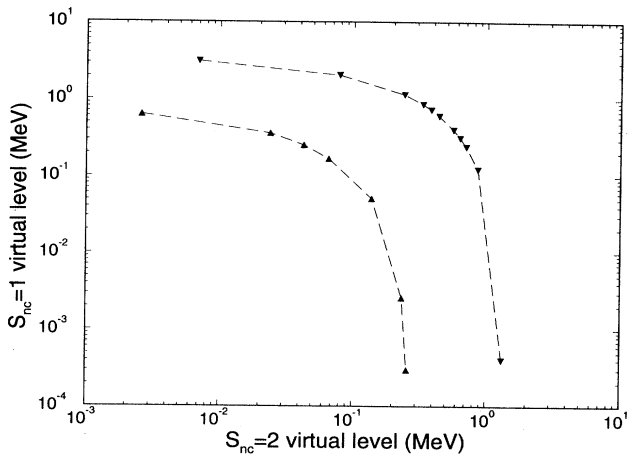

FIG. 4. The same as Fig. 2 for ^{19}B. The parameters correspond to the black triangles in Fig. 3 with the total energy equal to 0.45 MeV and 0.75 MeV. (The curves are obtained by varying γ_s.)

value for ^{19}B. This is consistent with $l_c = l_{nn} = s_{nn} = 0$, which normally would be the state of lowest energy in our three-body calculation. The two-neutron separation energy of ^{19}B is estimated to be 500±450 keV , see Ref. [20], and could in fact be anything below 1 MeV. Therefore we vary the energy along lines relating the neutron-core resonance energies by $E(d_{5/2}) = xE(s_{1/2})$, where x then is a number between 0 and ∞. Varying V_s and V_d we obtain the total three-body energy shown in Fig. 3 as a function of $E(s_{1/2})$ for several values of x. The p waves are not included in the allowed configuration space. This is equivalent to a choice of p-strength V_p, which places the p states at high positive energies. The spin orbit strength $V_{so}^{(d)} = -10$ MeV and the spin splitting parameter $\gamma_s = 0$ are kept constant in the calculation. The starting point is $V_s = -7.87$ MeV or $V_s = -7.40$ MeV corresponding to a virtual s state at 50 keV or 100 keV, respectively. The total three-body energy decreases almost linearly with increasing resonance energies for all x values and remains in all the cases considered within the limits of the estimate.

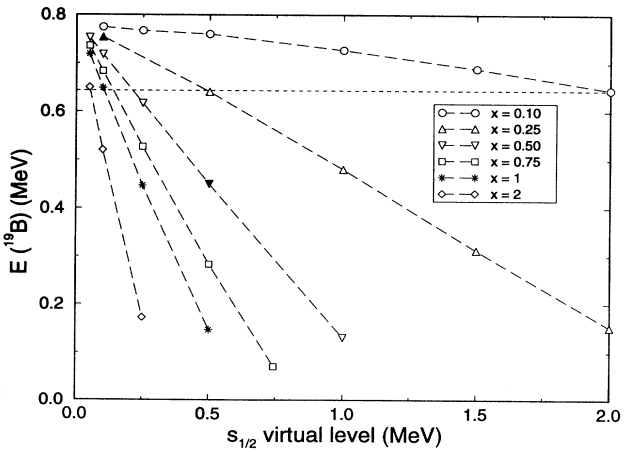

FIG. 3. The total energy of ^{19}B as function of the energy $E(s_{1/2})$ of the second virtual s state. The energy of the $d_{5/2}$ resonance in the neutron-core system is given by $E(d_{5/2}) = xE(s_{1/2})$ where x is constant along the curves. The parameters in the calculations are $V_{so}^{(d)} = -10$ MeV and $\gamma_s = 0$ while V_s and V_d are varied.

The total binding energies for the black triangles in Fig. 3 are around 0.45 MeV and 0.75 MeV. The effect of spin splitting in the s state is now investigated by increasing γ_s from zero while keeping the other parameters at values corresponding to these points. The strengths of the two potentials for a total spin of $s_c \pm 1/2$ are proportional to the related expectation values $\langle 1 + \gamma_s \mathbf{s}_c \cdot \mathbf{s}_n \rangle$, which, respectively, is $1 + \gamma_s s_c/2$ or $1 - \gamma_s(s_c + 1)/2$, see Eq. (14). The effective radial three-body potential is for small ρ a linear combination of these two two-body potentials with their respective statistical weights and it converges for large ρ toward the hyperspherical spectrum, i.e., values independent of the potential. This radial potential is consequently almost independent of γ_s and the resulting three-body energy is then also almost independent of γ_s. The connection between the energies of the two virtual s states corresponding to the spins $s_{nc} = 1, 2$ of the neutron-core system is shown in Fig. 4 as a function of γ_s for interaction parameters corresponding to the black triangles in Fig. 3. The qualitative behavior is similar to that of Fig. 2, since the total energy remains approximately unchanged.

IV. ANGULAR EIGENVALUE EQUATIONS FOR S STATES

As seen from Eq. (8) the angular eigenfunction $\lambda(\rho)$ is essentially an effective potential determined by Eq. (5). The generalized angular functions $\Phi_n^{(i)}(\rho, \Omega_i)$ is a sum of components with different angular momenta of the subsystems coupled to the total angular momentum. The

radial equations at large ρ do not couple neither these components nor those belonging to different Jacobi coordinates with the important exception of the states with zero two-body orbital angular momentum. These s states are often essential components in low-lying states of interest and we furthermore only introduced the spin splitting in s states. We shall therefore first concentrate on s states where the angular dependence in Eq. (4) is reduced to contain only α.

The spin dependence of the ith component of the total wave function in Eq. (2) is denoted $\chi_s^{(i)}$, where $\mathbf{s}$ is the intermediate spin obtained by coupling of the spins ($\mathbf{s}_j$ and $\mathbf{s}_k$) of particles j and k. The spin $\mathbf{s}$ is afterward coupled to $\mathbf{s}_i$ to give the spin of the core $\mathbf{s}_c$ which in our case equals the total spin of the system. For each channel the angular part can then be written as

$$\Phi^{(1)}(\rho,\alpha_1) = \frac{\phi_0^{(1)}(\rho,\alpha_1)}{\sin 2\alpha_1}\chi_0^{(1)}, \tag{15}$$

$$\Phi^{(2)}(\rho,\alpha_2) = \frac{\phi^{(2)}_{s_c-1/2}(\rho,\alpha_2)}{\sin 2\alpha_2}\chi^{(2)}_{s_c-1/2} + \frac{\phi^{(2)}_{s_c+1/2}(\rho,\alpha_2)}{\sin 2\alpha_2}\chi^{(2)}_{s_c+1/2}, \tag{16}$$

$$\Phi^{(3)}(\rho,\alpha_3) = \frac{\phi^{(3)}_{s_c-1/2}(\rho,\alpha_3)}{\sin 2\alpha_3}\chi^{(3)}_{s_c-1/2} + \frac{\phi^{(3)}_{s_c+1/2}(\rho,\alpha_3)}{\sin 2\alpha_3}\chi^{(3)}_{s_c+1/2}, \tag{17}$$

where the channel i=1 is defined by $\mathbf{x}$ between the two neutrons and where $\phi_s^{(i)}$ is the spatial part of the wave function related to $\chi_s^{(i)}$. Since the total wave function must be antisymmetric under interchanging of the two neutrons we have $\phi^{(3)}_{s_c-1/2} = \phi^{(2)}_{s_c-1/2}$ and $\phi^{(3)}_{s_c+1/2} = -\phi^{(2)}_{s_c+1/2}$.

Substituting Eqs. (15)–(17) into Eq. (5) with $i = 1, 2$ and subsequent multiplication from the left by $\chi_0^{(1)}$, $\chi^{(2)}_{s_c-1/2}$, and $\chi^{(2)}_{s_c+1/2}$ we obtain the following set of equations for the functions $\phi_0^{(1)}(\rho,\alpha_1)$, $\phi^{(2)}_{s_c-1/2}(\rho,\alpha_2)$, and $\phi^{(2)}_{s_c+1/2}(\rho,\alpha_2)$:

$$\left(-\frac{1}{\sin 2\alpha_1}\frac{\partial^2}{\partial\alpha_1^2}\sin 2\alpha_1 - \tilde{\lambda}(\rho)\right)\frac{\phi_0^{(1)}(\rho,\alpha_1)}{\sin 2\alpha_1} + \rho^2 v_{nn}(\rho\sin\alpha_1)\left[\frac{\phi_0^{(1)}(\rho,\alpha_1)}{\sin 2\alpha_1} + C_1\frac{\phi^{(2)}_{s_c-1/2}(\rho,\alpha_2)}{\sin 2\alpha_2} + C_2\frac{\phi^{(2)}_{s_c+1/2}(\rho,\alpha_2)}{\sin 2\alpha_2} + C_1\frac{\phi^{(2)}_{s_c-1/2}(\rho,\alpha_3)}{\sin 2\alpha_3} + C_2\frac{\phi^{(2)}_{s_c+1/2}(\rho,\alpha_3)}{\sin 2\alpha_3}\right] = 0, \tag{18}$$

$$\left(-\frac{1}{\sin 2\alpha_2}\frac{\partial^2}{\partial\alpha_2^2}\sin 2\alpha_2 - \tilde{\lambda}(\rho)\right)\frac{\phi^{(2)}_{s_c-1/2}(\rho,\alpha_2)}{\sin 2\alpha_2} + \rho^2\,\langle\chi^{(2)}_{s_c-1/2}|v_{nc}(\rho\sin\alpha_2)|\chi^{(2)}_{s_c-1/2}\rangle \times\left[C_1\frac{\phi_0^{(1)}(\rho,\alpha_1)}{\sin 2\alpha_1} + \frac{\phi^{(2)}_{s_c-1/2}(\rho,\alpha_2)}{\sin 2\alpha_2} + C_3\frac{\phi^{(2)}_{s_c-1/2}(\rho,\alpha_3)}{\sin 2\alpha_3} - C_4\frac{\phi^{(2)}_{s_c+1/2}(\rho,\alpha_3)}{\sin 2\alpha_3}\right] = 0, \tag{19}$$

$$\left(-\frac{1}{\sin 2\alpha_2}\frac{\partial^2}{\partial\alpha_2^2}\sin 2\alpha_2 - \tilde{\lambda}(\rho)\right)\frac{\phi^{(2)}_{s_c+1/2}(\rho,\alpha_2)}{\sin 2\alpha_2} + \rho^2\,\langle\chi^{(2)}_{s_c+1/2}|v_{nc}(\rho\sin\alpha_2)|\chi^{(2)}_{s_c+1/2}\rangle \times\left[C_2\frac{\phi_0^{(1)}(\rho,\alpha_1)}{\sin 2\alpha_1} + \frac{\phi^{(2)}_{s_c+1/2}(\rho,\alpha_2)}{\sin 2\alpha_2} - C_4\frac{\phi^{(2)}_{s_c-1/2}(\rho,\alpha_3)}{\sin 2\alpha_3} - C_3\frac{\phi^{(2)}_{s_c+1/2}(\rho,\alpha_3)}{\sin 2\alpha_3}\right] = 0, \tag{20}$$

where $v_{ij}(x) = V_{ij}(x/a_{ij})2m/\hbar^2$, $a_{jk} = [m_j m_k/(m(m_j+m_k))]^{1/2}$, $\tilde{\lambda}(\rho) = \lambda(\rho)+4$, and where we used that the neutron-neutron interaction ($v_{nn} = v_{23}$) is spin independent for s waves and that the neutron-core interaction ($v_{nc} = v_{12} = v_{13}$) is diagonal in spin space. The coefficients C_i, i=1,2,3,4 depend on the spin of the core, and take the values

$$\begin{aligned}
C_1 &= \langle\chi_0^{(1)}|\chi^{(2)}_{s_c-1/2}\rangle = \langle\chi_0^{(1)}|\chi^{(3)}_{s_c-1/2}\rangle \\
&= -\sqrt{s_c/(2s_c+1)}, \\
C_2 &= \langle\chi_0^{(1)}|\chi^{(2)}_{s_c+1/2}\rangle = -\langle\chi_0^{(1)}|\chi^{(3)}_{s_c+1/2}\rangle \\
&= \sqrt{(s_c+1)/(2s_c+1)}, \\
C_3 &= \langle\chi^{(2)}_{s_c-1/2}|\chi^{(3)}_{s_c-1/2}\rangle = \langle\chi^{(2)}_{s_c+1/2}|\chi^{(3)}_{s_c+1/2}\rangle \\
&= -1/(2s_c+1), \\
C_4 &= \langle\chi^{(2)}_{s_c-1/2}|\chi^{(3)}_{s_c+1/2}\rangle = -\langle\chi^{(2)}_{s_c+1/2}|\chi^{(3)}_{s_c-1/2}\rangle \\
&= \sqrt{4s_c(s_c+1)}/(2s_c+1). \qquad (21)
\end{aligned}$$

Equations (19) and (20) are identical to the ones obtained by substituting Eqs. (15)–(17) into Eq. (5) with $i=3$ and the subsequent multiplication from the left by $\chi^{(3)}_{s_c-1/2}$ and $\chi^{(3)}_{s_c+1/2}$.

The three spatial wave functions $\phi_0^{(1)}$ and $\phi^{(2)}_{s_c\pm1/2}$ are now for each ρ determined by Eqs. (18)–(20) and the following boundary conditions:

$$\begin{aligned}
\phi_0^{(1)}(\rho,\alpha=0) &= \phi_0^{(1)}(\rho,\alpha=\pi/2) = \phi^{(2)}_{s_c\pm1/2}(\rho,\alpha=0) \\
&= \phi^{(2)}_{s_c\pm1/2}(\rho,\alpha=\pi/2) = 0. \qquad (22)
\end{aligned}$$

For $\rho = 0$ Eqs. (18)–(20) clearly decouple and the solutions are

$$\phi^{(2)}_{s_c\pm1/2}(\rho=0,\alpha) = \phi_0^{(1)}(\rho=0,\alpha) \propto \sin(2n\alpha),$$

$$n = 1,2,3,\ldots \qquad (23)$$

and the eigenvalues are given by

$$\begin{aligned}
&\lambda_0 \equiv \lambda(\rho=0) = \tilde{\lambda}(\rho=0) - 4 = K(K+4), \\
&K = 2n-2, \qquad (24)
\end{aligned}$$

which is the well-known hyperspherical spectrum.

The behavior of λ for small ρ values can now be obtained in first-order perturbation theory. The easiest is to add the three equations in Eqs. (18)–(20) and thereby obtain the equivalent Schrödinger equation, which in turn then gives the following first-order correction to λ_0:

$$\begin{aligned}
\lambda(\rho) = \lambda_0 + \rho^2 \Bigg[& v_{nn}(\rho=0) \\
&+ \frac{2s_c}{2s_c+1}\,\langle\chi^{(2)}_{s_c-1/2}|v_{nc}(\rho=0)|\chi^{(2)}_{s_c-1/2}\rangle \\
&+ \frac{2s_c+2}{2s_c+1}\,\langle\chi^{(2)}_{s_c+1/2}|v_{nc}(\rho=0)|\chi^{(2)}_{s_c+1/2}\rangle \Bigg], \qquad (25)
\end{aligned}$$

where we used the spin independence of the neutron-neutron interaction. Equation (25) reduces for vanishing core-spin $s_c = 0$ and spin independent interactions to the usual small ρ expression, where only the sum of the interactions enters, see Ref. [7].

V. THE EFIMOV EFFECT

The large distance behavior of the λ values reflect characteristic properties of the three-body system and its subsystems. In particular the necessary and sufficient condition for the occurrence of the Efimov states is simply that $\lambda_\infty[\equiv \lambda(\rho\to\infty)]$ is smaller than -4 or equivalently $\tilde{\lambda} < 0$. Therefore eigenvalues and eigenfunctions for large ρ must be obtained from Eqs. (18)–(20) and we shall follow the procedure in Ref. [16].

The wave functions depending on α_k are first expressed in terms of the ith set of hyperspherical coordinates and the equations are subsequently integrated over the four angular variables $\mathbf{\Omega}_{x_k}$ and $\mathbf{\Omega}_{y_k}$. This amounts for s waves to the substitution formally expressed by the operator R_{ik} defined by

$$\begin{aligned}
R_{ik}\psi = &\frac{1}{\sin(2\varphi_{ik})}\frac{1}{\sin(2\alpha_i)} \\
&\times \int_{|\varphi_{ik}-\alpha_i|}^{\pi/2-|\pi/2-\varphi_{ik}-\alpha_i|} \sin(2\alpha_k)\psi(\rho,\alpha_k)d\alpha_k\,, \qquad (26)
\end{aligned}$$

where the transformation angle φ_{ik} is given by the masses as

$$\varphi_{ik} = \arctan\left((-1)^p\sqrt{\frac{m_j(m_1+m_2+m_3)}{m_i m_k}}\right), \qquad (27)$$

where $(-1)^p$ is the parity of the permutation $\{i,k,j\}$. The short ranges of the potentials confine α_k to be smaller than the range r_0 of the potential divided by ρ. [The precise definition of r_0 is given by $\rho^2 v_{nc}(r_0) = \tilde{\lambda}$.] The effect of the R operator is then for large ρ approximately given as

$$R_{ik}\psi \approx \frac{2\alpha}{\sin(2\varphi_{ik})}\psi(\rho,\varphi_{ik})\,. \qquad (28)$$

The wave function $\phi_0^{(1)}$ vanishes faster than $\phi^{(2)}_{s_c\pm1/2}$ provided the scattering lengths $a_\pm$ related to the two relative spin states of the neutron-core system both are larger than that of the neutron-neutron system. We can therefore omit Eq. (18) and neglect $\phi_0^{(1)}$ in Eqs. (19) and (20) and thereby for $\rho \gg r_0$ to first order in $\alpha_0 \equiv r_0/\rho$ obtain the simplified eigenvalue equations

$$\left(-\frac{\partial^2}{\partial\alpha_2^2}-\tilde{\lambda}(\rho)\right)\phi^{(2)}_{s_c-1/2}(\rho,\alpha_2)+\rho^2\ \langle\chi^{(2)}_{s_c-1/2}|v_{nc}(\rho\sin\alpha_2)|\chi^{(2)}_{s_c-1/2}\rangle$$

$$\left[\phi^{(2)}_{s_c-1/2}(\rho,\alpha_2)+\frac{2\alpha_2}{\sin 2\varphi}(C_3\phi^{(2)}_{s_c-1/2}(\rho,\varphi)-C_4\phi^{(2)}_{s_c+1/2}(\rho,\varphi))\right]=0\ , \quad (29)$$

$$\left(-\frac{\partial^2}{\partial\alpha_2^2}-\tilde{\lambda}(\rho)\right)\phi^{(2)}_{s_c+1/2}(\rho,\alpha_2)+\rho^2\ \langle\chi^{(2)}_{s_c+1/2}|v_{nc}(\rho\sin\alpha_2)|\chi^{(2)}_{s_c+1/2}\rangle$$

$$\left[\phi^{(2)}_{s_c+1/2}(\rho,\alpha_2)+\frac{2\alpha_2}{\sin 2\varphi}(-C_4\phi^{(2)}_{s_c-1/2}(\rho,\varphi)-C_3\phi^{(2)}_{s_c+1/2}(\rho,\varphi))\right]=0\ , \quad (30)$$

where $\varphi=\arctan\sqrt{A_c(A_c+2)}$ is given in terms of the nucleon number A_c of the core.

We now proceed by dividing the α_2 space into two regions I and II. In region I ($\alpha_2>\alpha_0=r_0/\rho$), where the potential is negligibly small, the solutions to the previous equations are

$$\phi^{(2,\mathrm{I})}_{s_c\pm1/2}(\rho,\alpha_2)\propto\sin\left[\left(\alpha_2-\frac{\pi}{2}\right)\sqrt{\tilde{\lambda}}\right]\ , \quad (31)$$

where we have imposed that the solution has to vanish at the boundary $\alpha_2=\pi/2$.

In region II ($\alpha_2<\alpha_0$), where $\tilde{\lambda}/\rho^2$ is negligibly small, we have two inhomogeneous differential equations with the solutions:

$$\phi^{(2,\mathrm{II})}_{s_c-1/2}(\rho,\alpha_2)$$

$$=u_-(\rho\alpha_2)-\frac{2\alpha_2}{\sin 2\varphi}[C_3\phi^{(2,\mathrm{I})}_{s_c-1/2}(\rho,\varphi)$$
$$-C_4\phi^{(2,II)}_{s_c+1/2}(\rho,\varphi)]\ , \quad (32)$$

$$\phi^{(2,\mathrm{II})}_{s_c+1/2}(\rho,\alpha_2)$$

$$=u_+(\rho\alpha_2)-\frac{2\alpha_2}{\sin 2\varphi}[-C_4\phi^{(2,\mathrm{I})}_{s_c-1/2}(\rho,\varphi)$$
$$-C_3\phi^{(2,\mathrm{I})}_{s_c+1/2}(\rho,\varphi)]\ , \quad (33)$$

where the inhomogeneous solutions, proportional to α_2, easily are found due to the linear dependence of α_2. The homogeneous solutions $u_\pm(\rho\alpha_2)$ are the wave functions describing the state of zero energy in their respective potentials $\langle\chi^{(2)}_{s_c\pm1/2}|v_{nc}(\rho\alpha_2)|\chi^{(2)}_{s_c\pm1/2}\rangle$. Outside the range of the potential ($\rho\alpha_2>r_0$) these wave functions take the form $u_\pm(\rho\alpha_2)\propto\rho\alpha_2+a_\pm$, where $a_\pm$ are the scattering lengths of the two neutron-core potentials corresponding to the two different spin couplings.

The eigenvalue equation for $\tilde{\lambda}$ now arises by matching of the derivative of the logarithm of the solutions at the division point $\alpha_2=\alpha_0=r_0/\rho$. Keeping only the lowest order in r_0/ρ, and assuming that both scattering lengths are much larger than r_0 ($a_\pm\gg r_0$), we finally obtain

$$\tilde{\lambda}\cos^2\left(\frac{\pi}{2}\sqrt{\tilde{\lambda}}\right)+\frac{\rho^2}{a_-a_+}\sin^2\left(\frac{\pi}{2}\sqrt{\tilde{\lambda}}\right)+\frac{1}{2}\left(\frac{\rho}{a_-}+\frac{\rho}{a_+}\right)\sqrt{\tilde{\lambda}}\sin(\pi\sqrt{\tilde{\lambda}})$$
$$+\frac{1}{2s_c+1}\left(\frac{\rho}{a_-}-\frac{\rho}{a_+}\right)\frac{2}{\sin 2\varphi}\sin\left(\frac{\pi}{2}\sqrt{\tilde{\lambda}}\right)\sin\left[\left(\varphi-\frac{\pi}{2}\right)\sqrt{\tilde{\lambda}}\right]-\frac{4}{\sin^2 2\varphi}\sin^2\left[\left(\varphi-\frac{\pi}{2}\right)\sqrt{\tilde{\lambda}}\right]=0\ . \quad (34)$$

The dependence on the core-spin s_c appears only through the scattering lengths $a_\pm$ and the parameter $C_3=-1/(2s_c+1)$.

When one or both of the scattering lengths are finite and negative, which means that at least one bound state exists in the neutron-core subsystem, the lowest $\tilde{\lambda}$ eigenvalue diverges as $-\rho^2/a^2$, where a is the scattering length for the channel of strongest binding. When both $a_\pm$ are positive or infinitely large, we can distinguish between three different cases. In the first case both a_+ and a_- are infinitely large. Then by keeping only the leading order, Eq. (34) reduces to

$$\tilde{\lambda}\cos^2\left(\frac{\pi}{2}\sqrt{\tilde{\lambda}}\right)-\frac{4}{\sin^2 2\varphi}\sin^2\left[\left(\varphi-\frac{\pi}{2}\right)\sqrt{\tilde{\lambda}}\right]=0\ , \quad (35)$$

which for ^{11}Li, where $\varphi=\arctan\sqrt{11\times9}$, has the lowest solution at $\tilde{\lambda}=-0.00545$. This value gives rise to an ef-

fective attractive potential in the radial equation, Eq. (8), given by $-0.25545/\rho^2$, which results in an infinite number of bound states. This number is independent of the core-spin s_c, and the only dependence on the nucleus is contained in the angle φ, see Eq. (27).

In the opposite limit, where ρ is large compared to both scattering lengths, i.e., $a_\pm \ll \rho$, the leading order approximation of Eq. (34) is simply

$$\sin^2\left(\frac{\pi}{2}\sqrt{\tilde{\lambda}}\right) = 0 \tag{36}$$

and the hyperspherical spectrum is recovered, i.e., $\tilde{\lambda}-4 = K(K+4), K = 0,2,4,\ldots$.

The last case is characterized by one small and one large scattering length compared to ρ, i.e., $0 < a_- \ll \rho \ll a_+$, or $0 < a_+ \ll \rho \ll a_-$. Now Eq. (34) reduces to leading order to the form

$$\sin\left(\frac{\pi}{2}\sqrt{\tilde{\lambda}}\right)\left\{\sqrt{\tilde{\lambda}}\cos\left(\frac{\pi}{2}\sqrt{\tilde{\lambda}}\right)\right.$$

$$\left.\pm\frac{1}{2s_c+1}\frac{2}{\sin 2\varphi}\sin\left[\left(\varphi-\frac{\pi}{2}\right)\sqrt{\tilde{\lambda}}\right]\right\} = 0\,, \tag{37}$$

where the $\pm$ signs appear for $a_\mp \ll \rho \ll a_\pm$. This equation is independent of $a_\pm$ and it has never any negative solutions. The lowest positive solutions for ^{11}Li are $\tilde{\lambda} = 0.702627$ and $\tilde{\lambda} = 1.34930$, respectively, when $a_- \ll \rho \ll a_+$ and $a_+ \ll \rho \ll a_-$. Since $\tilde{\lambda}$ always is positive this means that the barrier in the radial equation $[(\tilde{\lambda}-1/4)/\rho^2]$ never can give rise to the Efimov effect. This reflects the fact that infinitely many bound states only occur when at least two of the subsystems have infinitely large scattering lengths. If this extreme effect should be present both $a_\pm$ must be infinitely large.

The behavior of the $\tilde{\lambda}$ function is summarized in Fig. 5, where the lowest $\tilde{\lambda}$ for ^{11}Li is shown. The scattering lengths have been chosen to be 10^2 fm and 10^7 fm, and the dashed (solid) line corresponds to $a_- < a_+$ ($a_+ < a_-$). When both a_- and a_+ are much larger than ρ, both curves converge to the same value of $\tilde{\lambda} = -0.00545$. In the opposite limit where ρ is larger than both scattering lengths, the curves both approach the value 4 corresponding to the lowest level of the hyperspherical spectrum. In the intermediate region, where ρ is much larger than one of the scattering lengths and much smaller than the other, $\tilde{\lambda}$ has a flat region. The constant value depends in this case only on which of the scattering lengths is larger than the other, but not on the specific values of a_- and a_+. These $\tilde{\lambda}$ values are shown as dashed lines in the figure.

It is important to emphasize that the conditions for the appearance of the Efimov states become more restrictive for a finite spin of the core. In principle, the effect appears when at least two of the binary subsystems have extremely large scattering lengths. We have seen above that both the possible couplings of the neutron-core spin states for halo nuclei must correspond to extremely large scattering lengths. If only one of the scattering lengths

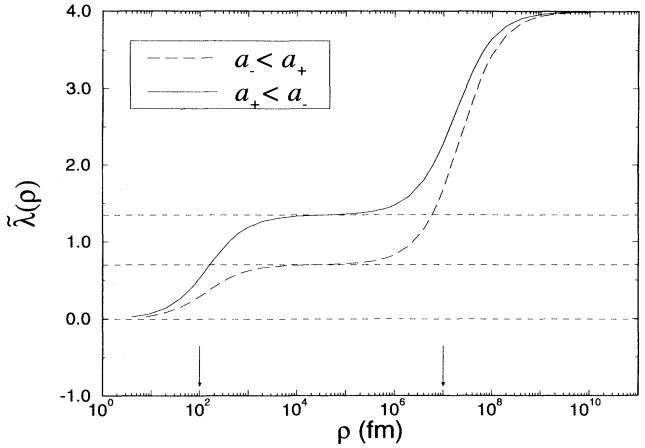

FIG. 5. Large distance behavior of the angular eigenvalue $\tilde{\lambda}$ as function of ρ for ^{11}Li. The scattering lengths (marked by the vertical arrows) are $a_- = 10^2$ fm and $a_+ = 10^7$ fm for the dashed line and $a_+ = 10^2$ fm and $a_- = 10^7$ fm for the solid line. The horizontal dashed lines correspond to the various limiting values described in the text.

is very large the λ function is not low enough to permit many bound states, i.e., occurrence of the Efimov effect. However, these conclusions do not affect halo nuclei with zero core spin. It should still be remembered that the most promising place in nuclei to look for the Efimov effect would be in a system, where one neutron is added to a pronounced one-neutron halo nucleus with zero core spin [7].

VI. SPATIAL STRUCTURE

The angular eigenvalues λ are the effective radial potentials. The spectrum is therefore decisive for the spatial structure of the system. In Fig. 6 is shown an example for interaction parameters corresponding to the square in Fig. 1, i.e., realistic values for ^{11}Li. The beginning of the hyperspherical spectrum $[K(K+4), K = 0,2,4\ldots]$ is seen at both $\rho = 0$ and at $\rho = \infty$. The lowest level decreases from zero at $\rho = 0$, goes through a minimum and returns back to zero at infinity. The return to zero at large distances means that none of the two-body interactions is able to hold bound states. The negative pocket at smaller distances signifies an attraction in the total three-body system. The attraction is in this case able to hold the system in a bound state although no binary subsystem is bound.

The angular structure corresponding to the eigenvalue spectrum is conveniently discussed in the Jacobi coordinate set where $\mathbf{x}$ is the vector between the two neutrons. The components of the wave function for $\rho = 0$ and $\rho = \infty$ corresponds to $(l_{nn}, l_c, L, s_{nn}, s_c, S) = (0,0,0,0,3/2,3/2)$ for the lowest level. The fivefold degeneracy of the $K = 2$ levels corresponds to the angular components $(l_{nn}, l_c, L, s_{nn}, s_c, S) = (0,0,0,0,3/2,3/2)$ with one node, $(1,1,0,1,3/2,3/2)$ and the three levels $(1,1,1,1,3/2,S)$ with $S = 1/2, 3/2, 5/2$.

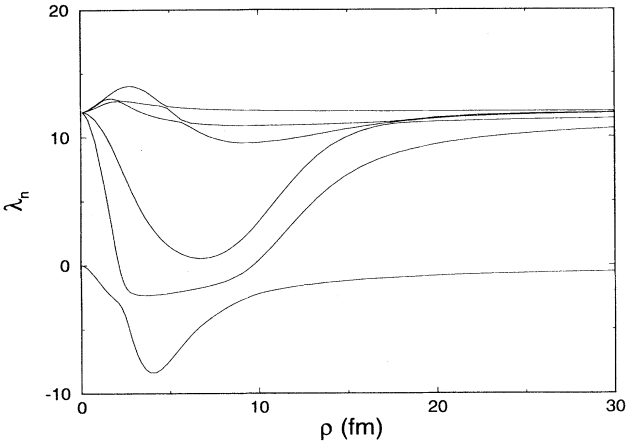

FIG. 6. The angular eigenvalues as function of the radial coordinate ρ for interaction parameters corresponding to the diamond on Fig. 1, i.e, ^{11}Li. Only antisymmetric states in the neutron-neutron exchange are exhibited.

The usual measure of the size of the system is the mean square radius, which for A_c nucleons in the core is given by

$$R^2_{\rm RMS} = \frac{A_c}{A_c+2} R^2_{\rm RMS}({\rm core}) + \frac{1}{A_c+2}\langle\rho^2\rangle, \qquad (38)$$

where $R^2_{\rm RMS}$ and $R^2_{\rm RMS}$(core) are mean square radii of the respective systems and the mean square of the hyperradius is given by $\langle\rho^2\rangle = A_c\langle r_c^2\rangle + 2\langle r_n^2\rangle$, where r_c and r_n are core and neutron coordinates measured from the center of mass of the total system.

In Fig. 7 we show the mean square radii along the curves in Figs. 2 and 4 as functions of energy of one of the virtual s states. Clearly this measure of the extension of the system is essentially independent of the spin splitting in all cases. This is due to the fact that the spin splitting gives rise to very small changes of the angular eigenvalue spectrum. The lowest λ functions are indistinguishable at large distances and only small differences occur at the smaller distances, where the wave function has small contributions.

However, the size depends both on the binding energy and the amount of higher angular momentum states in the neutron-core motion. For a given binding energy, the energy of the virtual s state decreases with increasing s-state content in the neutron-core subsystem, and then the spatial extension of the system increases due to the smaller centrifugal barrier. The essential parameter is the amount of s wave in the relative neutron-core motion. The variation of the root mean square radius of ^{11}Li and ^{19}B as functions of the s-wave probability alone is shown in Fig. 8. The white circles represent the variation of the radius for ^{11}Li along the curve in Fig. 1. The black circles represent the same variation for ^{19}B, but along the horizontal dashed line in Fig. 3, which corresponds to a constant energy of around 0.65 MeV. The resulting almost linear dependence for ^{11}Li is varying within limits consistent with both computations [8] and the recent interpretation [$R_{\rm RMS}(^{11}{\rm Li}) = 3.1 \pm 0.3$ fm] of the measured reaction cross sections [21].

In the ground state the ratio between the weights of the spin split s waves are predefined by the symmetry constraint in such a way that the parametrization in Eq. (14) makes the λ values nearly independent of γ_s. The resulting spatial three-body structure is therefore independent of the spin splitting provided the total energy and thereby the total s-state occupation probability remains unchanged. Any observable for the three-body system

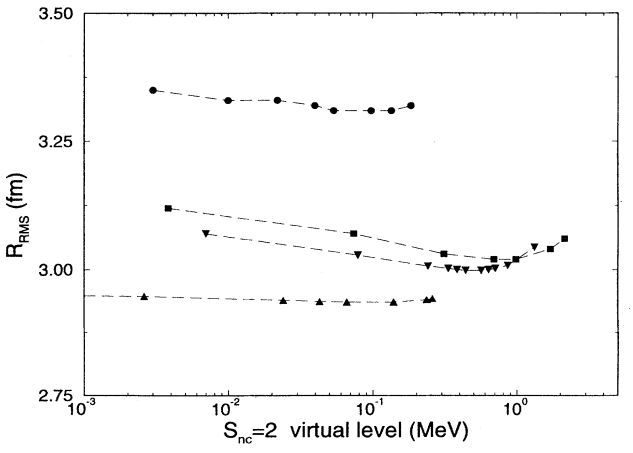

FIG. 7. The root mean square radius of ^{11}Li and ^{19}B as functions of the energy of one of the virtual s states for interaction parameters corresponding to the curves in Figs. 2 and 4. The squares, circles, and triangles have the same meaning as in those figures.

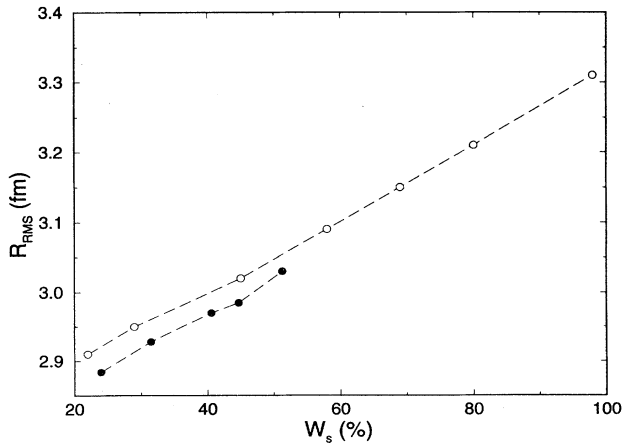

FIG. 8. The root mean square radii of ^{11}Li (open circles) and ^{19}B (black circles) as functions of the s-state admixture in the neutron-core channel. The core radii are $R_{\rm RMS}(^9{\rm Li}) = 2.32$ fm and $R_{\rm RMS}(^{17}{\rm B}) = 2.65$ fm, respectively. The interaction parameters correspond to the curve in Fig. 1 and the horizontal dashed line in Fig 3.

depending solely on the spatial structure is therefore unable to determine the spin splitting of the subsystem. Direct measurements of the neutron-core virtual states would of course in principle be able to give the information. However, angular momentum determination of these unstable nuclear states are needed.

A recent suggestion to determine the s-state admixture in the three-body ground state of ^{11}Li is highly relevant in this connection [22]. The idea is that in a nuclear break-up reaction the final-state interaction between the core and the neutron is decisive for the observed neutron momentum distribution. Low-lying virtual s states or equivalently strongly attractive s-state potentials will via the final-state interaction lead to a narrow momentum distribution [23]. A higher-lying s state or a p state with repulsive centrifugal barrier can only weakly influence the outgoing neutron. The necessary analyses require first of all the probability of finding the remaining neutron-core system in the low lying s state. For a non-negligible spin splitting this probability equals the probability of finding two occupied s states multiplied by the probability of survival (roughly the statistical weights independent of the spin splitting) of the low-lying state. Therefore information about the spin splitting may be obtained from these reactions.

VII. MAGNETIC DIPOLE MOMENT

Structural changes due to the spin splitting are most likely to show up in spin dependent observables. The natural first choice to study is the magnetic dipole moment, which in our three-body model is given by

$$\frac{\mu}{\mu_N} = \langle JM = J| \left(g_n \mathbf{s}_{nn} + g_c \mathbf{s}_c + Z_c \frac{2}{A_c + 2} \mathbf{l}_c \right)_z |JM = J\rangle, \tag{39}$$

where μ_N is the nuclear magneton, Z_c is the charge of the core, $\mathbf{l}_c$ is the orbital angular momentum of the core relative to the center of mass of the neutrons, J and M are the total angular momentum and its projection. The gyromagnetic factors are taken as $g_n = -3.8263$ for the neutron, $g_c = 3.4391/s_c$ for ^{11}Li, and the Schmidt value $g_c = 3.7928/s_c$ for ^{19}B. The nonvanishing matrix elements of the operator in Eq. (39) are then

$$\begin{aligned}
&\langle ((l_{nn} l_c) L (s_{nn} s_c) S; JJ| \ (\mathbf{s}_{nn})_z \ |(l_{nn} l_c) L (s_{nn} s_c) S'; JJ\rangle \\
&= (-1)^{J+L+S+S'+s_{nn}+s_c} \sqrt{J(2J+1)(2S+1)(2S'+1) s_{nn}(s_{nn}+1)(2s_{nn}+1)/(J+1)} \\
&\quad \times \begin{Bmatrix} S & 1 & S' \\ J & L & J \end{Bmatrix} \begin{Bmatrix} s_{nn} & 1 & s_{nn} \\ S' & s_c & S \end{Bmatrix},
\end{aligned} \tag{40}$$

where L is the total orbital angular momentum, l_{nn} is the orbital angular momentum of the two neutrons, S (S') is the total spin. The expression for the other two terms of the operator in Eq. (39) can be obtained, respectively, by exchange of $\mathbf{s}_c$ and $\mathbf{s}_{nn}$, and by additional exchanges of all spins and orbital angular momenta on the right-hand side of the equation.

The results of these formulas are given in Table I for both our examples of ^{11}Li and ^{19}B. The major contributions consistent with parity and angular momentum coupling rules are listed in the neutron-neutron Jacobi set of coordinates. All diagonal p-wave matrix elements except one are smaller than the s-wave matrix element. Since all these components are coupled in the three-body system one could expect that p-wave admixture will reduce the magnetic moment compared to the core value in contradiction with measurements for ^{11}Li [24]. However, the diagonal elements alone are very misleading due to the strong off-diagonal matrix elements given at the bottom of the table.

The result of direct numerical calculations for both ^{11}Li and ^{19}B show that the core value of the magnetic moment always is recovered and it is therefore insensitive both to the spin splitting and to the amount of p- or d-wave admixture. The reason is that the basic neutron-core components in the present three-body model for ^{11}Li are the $(s_{1/2})^2$ and $(p_{1/2})^2$ two-particle states. Both are fully occupied j shells of total angular momentum zero. Their contributions to the magnetic moment therefore must vanish and the off-diagonal elements are essential in this connection. We are therefore left with the core value. Our model also allows other configurations, which however turn out to be essentially unoccupied in the final wave function. For ^{19}B, where the p states are substituted by d states, we also recover the core value for the magnetic moment. The reason is that the new configuration $(d_{5/2})^2$ almost exclusively couples to the total spin zero and therefore also in this case only contributes insignificantly. Other components are apparently energetically too expensive.

The accuracy of the strict three-body model is relying on the assumption of an inert core. Thus core degrees of freedom must be included when improvements beyond the three-body model are requested. The most obvious

TABLE I. Diagonal contributions to the magnetic moment from two-body s and p states in the neutron-neutron Jacobi coordinate system. The total and core angular momenta and parities are given by $J^\pi = 3/2^-$ and $s_c^\pi = 3/2^-$. The nonvanishing off-diagonal matrix elements are shown at the bottom of the table.

No.	l_{nn}	l_c	L	s_{nn}	S	$\langle(\mathbf{s}_{nn})_z\rangle$	$\langle(\mathbf{s}_c)_z\rangle$	$\langle(\mathbf{l}_c)_z\rangle$	$\mu(^{11}\mathrm{Li})$	$\mu(^{19}\mathrm{B})$
1	0	0	0	0	3/2	0	3/2	0	$3.4391=\mu_c$	$3.7928=\mu_c$
2	1	1	0	1	3/2	2/5	11/10	0	0.99	1.25
3	1	1	1	1	1/2	−1/3	5/6	1/2	3.46	3.65
4	1	1	1	1	3/2	22/75	121/150	1/5	0.84	1.02
5	1	1	1	1	5/2	21/25	63/50	−3/10	−0.49	−0.19
6	1	1	2	1	1/2	1/5	−1/2	9/10	−1.42	−1.56
7	1	1	2	1	3/2	2/25	11/50	3/5	0.53	0.57
8	1	1	2	1	5/2	13/25	39/50	1/10	−0.15	0.04
		$\langle 2\|$	μ	$\|4\rangle$		0	0	$\sqrt{2/5}$	0.34	0.33
		$\langle 3\|$	μ	$\|4\rangle$		$-\sqrt{2/3}$	$-\sqrt{2/3}$	0	0.72	0.61
		$\langle 3\|$	μ	$\|6\rangle$		0	0	$-\sqrt{1/20}$	−0.12	−0.12
		$\langle 4\|$	μ	$\|5\rangle$		$-\sqrt{54}/25$	$-\sqrt{54}/25$	0	0.45	0.38
		$\langle 4\|$	μ	$\|7\rangle$		0	0	2/5	12/55	4/19
		$\langle 5\|$	μ	$\|8\rangle$		0	0	$\sqrt{21}/10$	0.25	0.24
		$\langle 6\|$	μ	$\|7\rangle$		$-\sqrt{2/5}$	$-\sqrt{2/5}$	0	0.97	0.82
		$\langle 7\|$	μ	$\|8\rangle$		$-3\sqrt{14}/25$	$-3\sqrt{14}/25$	0	0.69	0.58

modification for ^{11}Li is to allow an admixture of the only particle stable excited state, an angular momentum 1/2 state [14], into the 3/2 ground state of ^{9}Li. Since all matrix elements of the magnetic dipole operator in Eq. (39) vanish between states of different core spin, only the contributions in Table II are able to modify our previous results. Although we assumed an unchanged gyromagnetic factor for the core, it is rather obvious that any $s_c = 1/2$ admixture would further reduce the magnetic moment. A value of s_c larger than 3/2 is needed, but not available in the discrete spectrum of ^{9}Li. The effect of higher angular momentum neutron-core states and a j shell only partially occupied by the halo neutrons does not alter the conclusions above as seen from our example of ^{19}B.

VIII. EXCITED STATES OF ELECTRIC DIPOLE CHARACTER

The spectrum of excited states in halo nuclei is almost by definition limited to at most a few discrete states, but the continuum structure including resonances might also be interesting. The 1^- type of excitations, continuous or discrete, are for such nuclei expected to differ significantly from corresponding states in normal nuclei. The only excited state in ^{11}Be has the largest measured $B(E1)$ value to the ground state [25]. In general the dipole strength function is peaked at low excitation energies and it plays a dominant role in the analysis of Coulomb dissociation cross sections [1,26,27]. The peak

TABLE II. Diagonal contributions to the magnetic moment from two-body s and p states in the neutron-neutron Jacobi coordinate system. The total and core angular momenta and parities are given by $J^\pi = 3/2^-$ and $s_c^\pi = 1/2^-$. The nonvanishing off diagonal matrix elements are shown at the bottom of the table. The gyromagnetic factors of the core are, respectively, $g_c = 3.4391/1.5$ and $g_c = 3.7928/1.5$.

No.	l_{nn}	l_c	L	s_{nn}	S	$\langle(\mathbf{s}_{nn})_z\rangle$	$\langle(\mathbf{s}_c)_z\rangle$	$\langle(\mathbf{l}_c)_z\rangle$	$\mu(^{11}\mathrm{Li})$	$\mu(^{19}\mathrm{B})$
1	0	2	2	0	1/2	0	−3/10	9/5	0.29	0.19
2	2	0	2	0	1/2	0	−3/10	0	−0.69	−0.76
3	1	1	1	1	1/2	2/3	−1/6	1/2	−2.66	−2.71
4	1	1	2	1	1/2	−2/5	1/10	9/10	2.25	2.26
5	1	1	0	1	3/2	1	1/2	0	−2.68	−2.56
6	1	1	1	1	3/2	11/15	11/30	1/5	−1.86	−1.77
7	1	1	2	1	3/2	1/5	1/10	3/5	−0.21	−0.20
		$\langle 3\|$	μ	$\|4\rangle$		0	0	$1/\sqrt{20}$	0.12	0.12
		$\langle 3\|$	μ	$\|6\rangle$		$-2/\sqrt{45}$	$-2/\sqrt{45}$	0	0.46	0.39
		$\langle 4\|$	μ	$\|7\rangle$		−2/5	−2/5	0	0.61	0.52
		$\langle 5\|$	μ	$\|6\rangle$		0	0	$\sqrt{2/5}$	0.34	0.33
		$\langle 6\|$	μ	$\|7\rangle$		0	0	2/5	12/55	4/19

has even been suggested to be a new type of low-lying excitation mode for halo nuclei [28,29]. In any case it can be expected that these 1^- excitations are the lowest-lying excitations in halo nuclei.

When the total angular momentum as well as the spin of the core both are zero the major components in the wave function of the excited 1^-—state are most conveniently described in the neutron-neutron coordinate system. The angular momentum 1 and the negative parity can be made by $(l_{nn}, l_c, L, s_{nn}, s_c) = (0,1,1,0,0)$ and $(1,0,1,1,0)$ if we for simplicity exclude d and higher partial waves. The finite core spin now dictates the additional coupling of s_c to a total angular momentum of $J = s_c, s_c \pm 1$. The parity is still the opposite of the ground state.

For a core spin of 3/2 corresponding to ^{11}Li the total angular momenta are $J = 1/2, 3/2$, and $5/2$. They are shown in Fig. 9 as functions of the spin splitting parameter γ_s. The ground-state energy is also shown for comparison and as expected seen to be almost independent of the spin splitting. In contrast the energies of the excited states vary with γ_s. An increase is seen for $J = 1/2, 3/2$ and a decrease for $J = 5/2$. Crudely speaking the 1^--state consists of one neutron in an s state and the other neutron in a p state relative to the core. By selecting the lowest lying of the (spin split) s states the energy of the three-body state could therefore be expected to decrease with the energy of one of the s states in the neutron-core subsystem, i.e., as soon as $\gamma_s \neq 0$. However, the 1^- states have admixtures, determined by a complex interplay of several factors, of spin-split s waves different from the ground state. Due to the antisymmetry requirement it is impossible to construct a wave function with given total J and one neutron in the lowest neutron-core spin split s state and the other neutron in a p state. Both virtual s states are necessarily present. The $J = 5/2$ state has an excess of neutron-core states with angular momentum $s_{nc} = s_c + 1/2 = 2$, the $J = 1/2$ has analogously an excess of $s_{nc} = s_c - 1/2 = 1$ and the $J = 3/2$ state is somewhere in between.

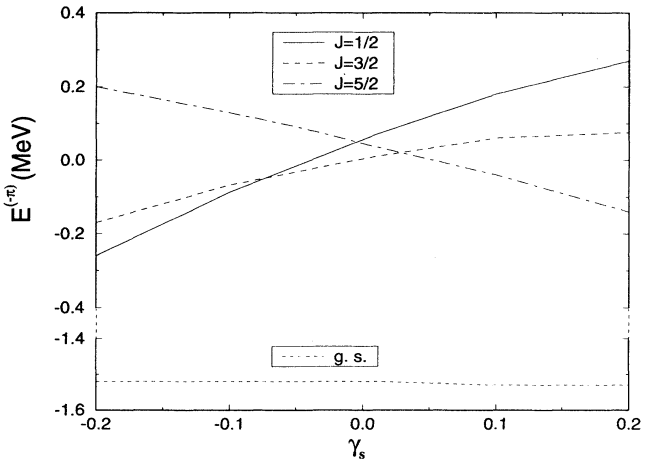

FIG. 9. The ground state and the excited 1^- levels as functions of the spin splitting parameter γ_s. The interaction parameters are $V_s = -8.5$, $V_p = -7.8$, and $V_{so}^{(p)} = 34.3$ MeV.

From the interaction in Eq. (14) we see that a negative value of $V_s\gamma_s$ implies that the energy of the neutron-core state with angular momentum $s_c + 1/2$ is lower than that of $s_c - 1/2$. In our specific case of $s_c = 3/2$ this corresponds for positive γ_s ($V_s < 0$) to a lower energy for the state of 2 than for that of 1. Thus the energy of the state with the largest content of 2 must exhibit the fastest decrease with γ_s. Therefore with increasing γ_s the $J = 5/2$ state necessarily becomes lowest in energy followed by the $J = 3/2$ state and with $J = 1/2$ as the highest. The details of the resulting energies are seen in Fig. 9. An increase of the ground-state energy would bring the excited spectrum into the continuum, but a similar structure would remain.

IX. SUMMARY AND CONCLUSION

We discuss in this paper the effects of a finite core spin on the structure of two-neutron halo nuclei. In the previous two papers in this series we established the general connections between size and binding energy for loosely bound three-body systems. The possible asymptotic (spatially extended and small energy) structures were characterized by the interactions between the constituent binary subsystems. The largest of the "particles" called the core is assumed to be inert and spinless and the corresponding degrees of freedom are frozen. When the core has a finite spin the two-body interaction between the core and another particle (typically a neutron) depends on the total spin of the two-body system. More complicated spin structures therefore seems to be possible even when the core still remains inert. This paper, number III in the series, is devoted to study effects of such spin couplings on the three-body system.

The recently developed method to solve the Faddeev equations is well suited for our purpose. We therefore first described the necessary ingredience of our procedure. The definitions and notation are then established in general and we proceed to consider the crucial two-body interactions. The neutron-neutron potential is needed in both relative s and p waves and since the spin structure is under investigation we also have to distinguish between the singlet and triplet states with the different total angular momenta. Low energy properties are still expected to be decisive and we construct therefore an interaction which reproduces the four phenomenologically extracted s- and p-wave scattering lengths and in addition the s-wave effective range. This is achieved by use of spin-spin, spin-orbit, and tensor terms with a common Gaussian radial dependence. The resulting effective low energy neutron-neutron interaction might also be useful in other connections.

The unknown neutron-core effective potential is also parametrized with a Gaussian radial shape. The minimum spin dependence includes a spin-orbit interaction and also the central interaction is allowed to be different in each of the relative orbital angular momentum channels. We furthermore for s waves include a term to dis-

tinguish between the possible couplings of the core and neutron spins and we choose the scalar product of these spins. The resulting interaction is now flexible enough to study the influence on the three-body system of the spin splitting and energy dependence of the resonances in the binary subsystems.

Equipped with an efficient method and the input properly parametrized we then explicitly write down the angular eigenvalue equations when only s waves are included. These states are often the most essential components in the solutions. We find analytically both small and large distance behavior of the angular eigenvalues. The conditions for the Efimov effect are simultaneously obtained and investigated in terms of scattering lengths for the two different spin couplings of the neutron-core subsystem. The extreme Efimov effect, where infinitely many bound states are present in the three-body system only occurs when both scattering lengths are infinitely large. Already the first of these excited states is very extended in space compared to the ranges of the potentials and the conditions for its presence is therefore interesting even when no other excited state exists. These conditions may conveniently be formulated in terms of bound state and virtual s-state energies of the neutron-core subsystem. Both the two spin couplings of $s_c \pm 1/2$ must correspond to energies between about -2 keV and 5 meV. Since the typical spin splitting of such s states is fractions of an MeV, the occurrence of the first Efimov state is extremely unlikely for a halo nucleus with a finite core spin.

The spatial structure of the three-body ground state turns out to be essentially independent of the spin splitting of the virtual s state. The reason is that either none or both s states are needed in one specific combination, if a total spin zero state has to be formed from the spins of the two neutrons. Any other combination has the wrong parity. On the other hand the spatial extension depends on the amount of s-state admixture as noted in previous publications and easily understood from the general behavior of states with higher angular momenta or higher hyperspherical quantum numbers.

The energy of the three-body ground state depends sensitively on the energies of the (spin split) virtual neutron-core s states, which constitute the components of the total system. The connection between the properties of the neutron-core system and the total three-body system depends strongly on the spin splitting. This may be exemplified by ^{10}Li and ^{11}Li, where a given s-state content in the ^{11}Li wave function requires a specific combination of the two virtual s states in ^{10}Li. If one is low lying the other energy must be high in order to compensate and lead to the observed total three-body binding energy. Thus, both virtual s states in ^{10}Li must be known, if the ^{11}Li-binding energy should be accounted for unambiguously.

The neutron-core s-state admixture in ^{11}Li is, as recently suggested, possible to extract from the measured momentum distributions in nuclear break-up reactions. In the sudden approximation, where one of the neutrons is removed instantaneously, there is a finite probability of finding the other neutron in the lowest-lying virtual s state. Due to the strong attraction this part of the wave function leads to a narrow observable momentum distribution.

The most obvious spin dependent observable is the magnetic dipole moment, which for ^{11}Li is found to be fairly close to the core value measured for ^{9}Li. The results of our strict three-body calculations are that the core value is reproduced independent of spin splitting and s-state admixture. The reason is that the spins of the two neutrons always couple to zero even when other possibilities are allowed.

The discrete or continuous spectrum of excited states of 1^-character on top of the ground state is of special interest for halo nuclei. One of the main components in the three-body wave function consists of one neutron in an s state and the other neutron in a p state relative to the core. Coupling of these angular momenta to 1 unit of $\hbar$ corresponds to an electric dipole excitation. More than one electric dipole excitation corresponding to different angular momenta is possible for finite core spin. The related hyperfine splitting of the $E1$ excitation leads to predictable structure in the continuum. Analyses of, for example, Coulomb dissociation cross sections may elucidate the structure of this 1^- excitation spectrum.

The excitation energy of such states may for a given total energy depend strongly on the spin splitting of the virtual s states. The reason is that the excited states are composed of mixtures of spin split s states different from that of the ground state. On average the lowest s state is preferred and the statistically weighted excitation energies therefore decrease when the energy of the lowest virtual s state approaches zero. The absolute value of this average depends on the energy of the p-state resonance.

In conclusion, we have investigated effects of finite core spin in halo nuclei. We found essentially unchanged spatial structure and magnetic dipole moments. Efimov states seem to be extremely unlikely in halo nuclei with finite core spin. The electric dipole excitations may depend rather strongly on the relative positions of the resonances and virtual states in the neutron-core subsystem. The spin splitting of the s states in the neutron-core system is decisive to understand the proper relation between the total three-body system and its subsystems. Our numerical examples concentrated on ^{11}Li (neutron-neutron-^{9}Li) and ^{19}B (neutron-neutron-^{17}B). These examples are used for general illustration, but they are useful in their own right as model computations for these nuclei.

ACKNOWLEDGMENTS

One of us (D.V.F.) acknowledges the support from the Danish Research Council and from INFN, Trento, Italy. E.G. was supported by Human Capital and Mobility Contract No. ERBCHBGCT930320.

[1] P.G. Hansen and B. Jonson, Europhys. Lett. **4**, 409 (1987).
[2] P.G. Hansen, Nucl. Phys. **A553**, 89c (1993).
[3] I. Tanihata, Nucl. Phys. **A522**, 275c (1991).
[4] K. Riisager, A.S. Jensen, and P. Møller, Nucl. Phys. **A548**, 393 (1992).
[5] D.V. Fedorov, A.S. Jensen, and K. Riisager, Phys. Lett. B **312**, 1 (1993).
[6] D.V. Fedorov, A.S. Jensen, and K. Riisager, Phys. Rev. C **49**, 201 (1994).
[7] D.V. Fedorov, A.S. Jensen, and K. Riisager, Phys. Rev. C **50**, 2372 (1994).
[8] M.V. Zhukov, B.V. Danilin, D.V. Fedorov, J.M. Bang, I.S. Thompson, and J.S. Vaagen, Phys. Rep. **231**, 151 (1993).
[9] J.-M. Richard and S. Fleck, Phys. Rev. Lett. **73**, 1464 (1994).
[10] L. Johannsen, A.S. Jensen, and P.G. Hansen, Phys. Lett. B **244**, 357 (1990).
[11] G.F. Bertsch and H. Esbensen, Ann. Phys. (N.Y.) **209**, 327 (1991).
[12] M.V. Zhukov, D.V. Fedorov, B.V. Danilin, J.S. Vaagen, and J.M. Bang, Nucl. Phys. **A529**, 53 (1991).
[13] J.M. Bang and I.J. Thompson, Phys. Lett. B **279**, 201 (1992); I.J. Thompson and M.V. Zhukov, Phys. Rev. C **49**, 1904 (1994).
[14] F. Ajzenberg-Selove, Nucl. Phys. **A490**, 1 (1988); **A506**, 1 (1990).
[15] H.G. Bohlen *et al.*, Z. Phys. A **344**, 381 (1993).
[16] D.V. Fedorov and A.S. Jensen, Phys. Rev. Lett. **71**, 4103 (1993); D.V. Fedorov, A.S. Jensen, and K. Riisager, *ibid.* **73**, 2817 (1994).
[17] J.H. Macek, J. Phys. B **1**, 831 (1968).
[18] T.K. Das, H.T. Coelho, and V.P. Brito, Phys. Rev. C **48**, 2201 (1993).
[19] O. Dumbrajs *et al.*, Nucl. Phys. **B216**, 277 (1983).
[20] G. Audi and A.H. Wapstra, Nucl. Phys. **A565**, 66 (1993).
[21] I. Tanihata *et al.*, Phys. Lett. B **287**, 307 (1992).
[22] M. Zinser *et al.*, Phys. Rev. Lett. (submitted).
[23] F. Barranco, E. Vigezzi, and R.A. Broglia, Phys. Lett. B **319**, 387 (1993).
[24] ISOLDE Collaboration, E. Arnold, J. Bonn, R. Gegenwart, W. Neu, R. Neugart, E.W. Otten, G. Ulm, and K. Wendt, Phys. Lett. B **197**, 311 (1987).
[25] D.J. Millener, J.W. Olness, and E.K. Warburton, Phys. Rev. C **28**, 497 (1983).
[26] Y. Suzuki and Y. Tosaka, Nucl. Phys. **A517**, 599 (1990).
[27] B.V. Danilin, I.J. Thompson, M.V. Zhukov, J.S. Vaagen, and J.M. Bang, Phys. Lett. B **333**, 299 (1994).
[28] S.A. Fayans, Phys. Lett. B **267**, 443 (1991).
[29] H. Esbensen and G.F. Bertsch, Nucl. Phys. **A542**, 310 (1992).